Progress In Electromagnetics Research C, Vol. 103, 137–153, 2020

Design of 4×4 Butler Matrix and Its Process Modeling Using Petri Nets for Phase Array Systems

Ved Prakash[1, *], Sonal Dahiya[1], Sunita Kumawat[2], and Priti Singh[1]

Abstract—Petri net is a mathematical and graphical tool used for analyzing the properties of parallel and concurrent system designs. Here, it is used for checking the process modeling of 4×4 Butler matrix fabricated on Rogers RO3210 and resonating in Ku band. Butler matrix is well suited for satellite and aircraft antenna applications as a feeding network for phase array systems. So, this basic feed design process of antennas is studied using Petri nets for better understating the designing process and removal of any deadlocks occurring during designing and feeding of antennas. It is accomplished by analyzing the behavioral and structural properties of Petri nets. A Butler matrix divides the power amplitude into four equal parts and provides a progressive phase difference of 45°. Therefore, its components, 0 dB coupler, 3 dB coupler, and phase shifters, have also been designed and simulated. After designing the components, firstly these components are joined to form a matrix design which is simulated and fabricated in ANSYS HFSS. Secondly, the designed structure is analyzed for structural and behavioral properties using Petri net's graphical and mathematical properties. After analyzing the process, the feed design can be modified further according to user requirements, and deadlock can be removed by checking the difference between the simulated and measured results of design. Likewise, here the matrix has been compared and found to be following the same pattern. The overall size of the matrix is $5.58 \times 7.43\,\text{cm}^2$, which is further suitable for the user's feeding requirements and applications.

1. INTRODUCTION

Antenna-array systems play a vital role in applications where high directivity of the antenna is in demand. This includes applications like wireless communication systems, radars, satellite communications, industrial and medical fields, multiple input and multiple output (MIMO) systems, etc. [1–4]. Beam-scanning systems require the user to provide beam to scan in a direction with low power consumption and simple algorithms. Butler matrix is one such method of feeding the antenna system at low cost, with simple circuits, lossless and uses minimum components. Recently, a lot of work has been done in the field of beam-scanning using Butler matrix. Most of the work focuses on the arrangement of the Butler matrix components or increasing the order of the matrix [5–10]. Recently, the matrix has also been evolved in the new fields of design like using substrate Integrated waveguide (SIW) technology, without phase shifters, odd order matrix, designing dual-band matrix, and their integration with antenna arrays [8, 10–16]. The performance of Butler matrix in terms of broadband matrix, wide scanning ability, and coverage has gained popularity, and a new approach without using phase shifters or flexible phase difference has also been applied in the recent years [17–20]. The main problem in designing Butler matrix is the attachment of its components and their impedance matching. However, conventionally the simplicity, ease of fabrication, and phase provided by the network are

Received 20 February 2020, Accepted 12 June 2020, Scheduled 30 June 2020
* Corresponding author: Ved Prakash (vprakash@ggn.amity.edu).
[1] Department of Electronics and Communication Engineering, Amity University Haryana, Gurugram, India. [2] Department of Applied Mathematics, Amity University Haryana, Gurugram, India.

the desirable parameters which differentiate every matrix. For analysis of the network design process, graph theory based techniques are also useful for behavioral and structural analysis of design process. Among them, Petri net (PN) is one of the most important tools for modelling graphically and analysing mathematically [21–23].

Petri net and its extensions like stochastic Petri net, fuzzy Petri nets, and other variants have evolved over the years and have many applications in all fields of engineering and sciences [24]. A wide survey of modeling techniques has been done based on both simulation and analytical modeling in communication network [21]. It is a model checking method through structural and behavioral properties like liveness, coverability, bounded ness, etc.

This paper introduces Petri nets modeling and analysis techniques used for verification and validation of design process. Before that, a 4×4 Butler matrix and its components are introduced for understanding the basic design process. Petri net is the most suitable graphical technique for representation like flowchart or block diagrams and is also useful for analysis of the mathematical properties [25, 26].

Butler matrix gives the theory and simulated diagrams of components (3-dB coupler, 0 dB coupler, and phase shifters) of the Butler matrix, and then these components are arranged in such a manner that the matrix divides power in four equal parts and provides a progressive phase difference of 45°. The 4×4 Butler matrix is designed and simulated on Rogers RO3210(tm) with dielectric constant of 10.2 and height of $h = 0.64$ mm, resonating at a frequency of 12.50 GHz. The simulation is done in ANSYS HFSS while properties and process modeling are done by Petri nets using PN-toolbox in MATLAB.

2. BUTLER MATRIX COMPONENTS DESIGN

The matrix is designed using transmission lines whose dimensions are calculated by Equation (1)

$$Z_o = \begin{cases} \dfrac{60}{\sqrt{\in}_{eff}} \ln\left[\frac{8h}{W} + \frac{W}{4h}\right], & \dfrac{W}{h} \leq 1 \\ \dfrac{120\pi}{\sqrt{\in}_{eff}\left[\dfrac{W}{h} + 1.393 + 0.667 \ln\left(\dfrac{W}{h} + 1.444\right)\right]}, & \frac{W}{h} > 1 \end{cases} \tag{1}$$

where W is the width of the transmission line, Z_o the characteristic impedance of the transmission line, and its standard value of 50 Ω is taken. The different components of the Butler matrix are 3-dB coupler, 0 dB coupler, and phase shifters. These are explained and simulated in the subsequent sections.

2.1. 3-dB Coupler

It is also called 90° quadrature coupler. It consists of four ports out of which one is input port,; two are output ports; and one is isolation port. The arrangement of the transmission line is such that powers at the output ports are equal in magnitude and 90° out of phase. The arrangement of the transmission line is shown in Figure 1.

Specifically, port P1 acts as the input port whereas ports P2 and P3 are the output ports where the powers are with same magnitude and out of phase by 90°. Port P4 acts as the isolation port. To design a 3 dB coupler, an arrangement of four transmission lines is done in such a way that the two horizontal lines have characteristic impedance as Z_o, and the vertical lines have impedance of $Z_o/\sqrt{2}$.

The values of the dimension width are calculated using the design Equation (1) and are found to be 0.6 mm for the characteristic impedance. Also, as seen from Figure 1, the width of the transmission line increases with decrease in the characteristic impedance $Z_o/\sqrt{2}$ and is calculated as 1.15 mm. These width dimensions are also used for the 0 dB coupler. The 3 dB coupler is designed in ANSYS HFSS to obtain the S-parameters and is shown in Figure 2.

It can be seen from Figure 2 that S_{11}, S_{21}, S_{31}, and S_{41} are −27.88 dB, −2.38 dB, −5.48 dB, and −40.71 dB, respectively. These results show that there is complete isolation between port 1 and port 4 while power is transferred to port 3 and port 4. The phase of the powers at the output ports is shown in Figure 3.

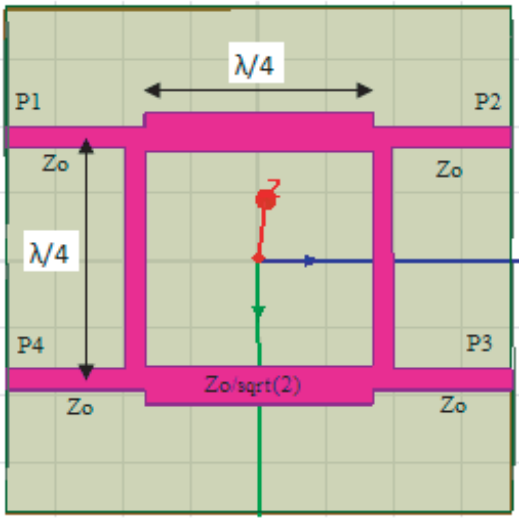

Figure 1. Layout of 3 dB coupler.

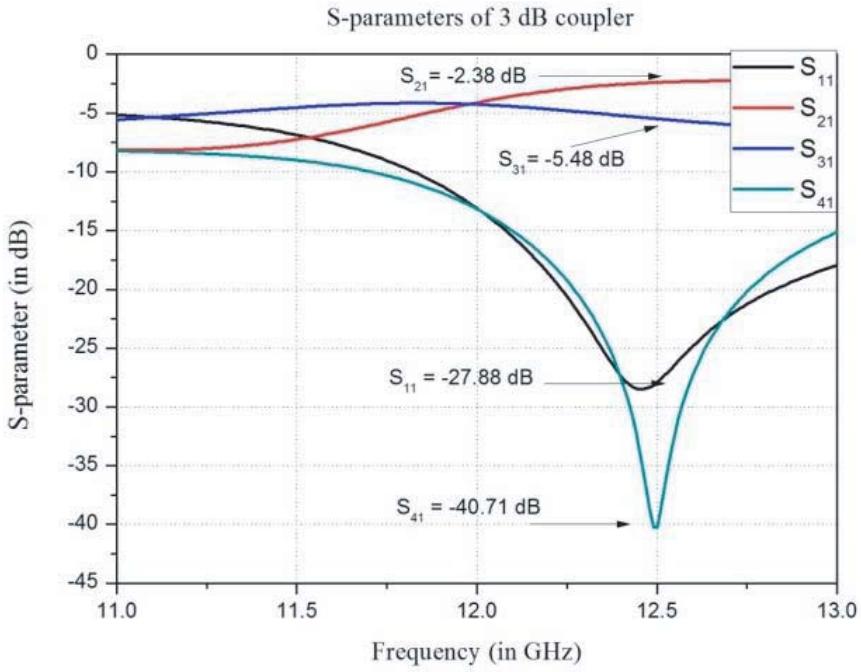

Figure 2. *S*-parameter of 3 dB coupler.

It can be seen from Figure 3 that S_{12} and S_{13} are $-102.03°$ and $-11.39°$, respectively, and thus give an exact phase difference of $-90.64°$ between the two ports, P2 and P3.

2.2. 0 dB Coupler

It is also called crossover and is realized by cascading two 3 dB couplers resulting in two input and two output ports. In a perfect design, every adjacent port is isolated, and power can be taken out from the left port. For example, port 1 is taken as the input port, then there will not be any power transferred to port 2 and port 4 which are its adjacent ports, and there will be power output from port 3 only. The impedances of the transmission are calculated from Equation (1), and then impedance matching is done. Figure 4 shows the arrangement of a 0 dB coupler made by using a microstrip transmission line.

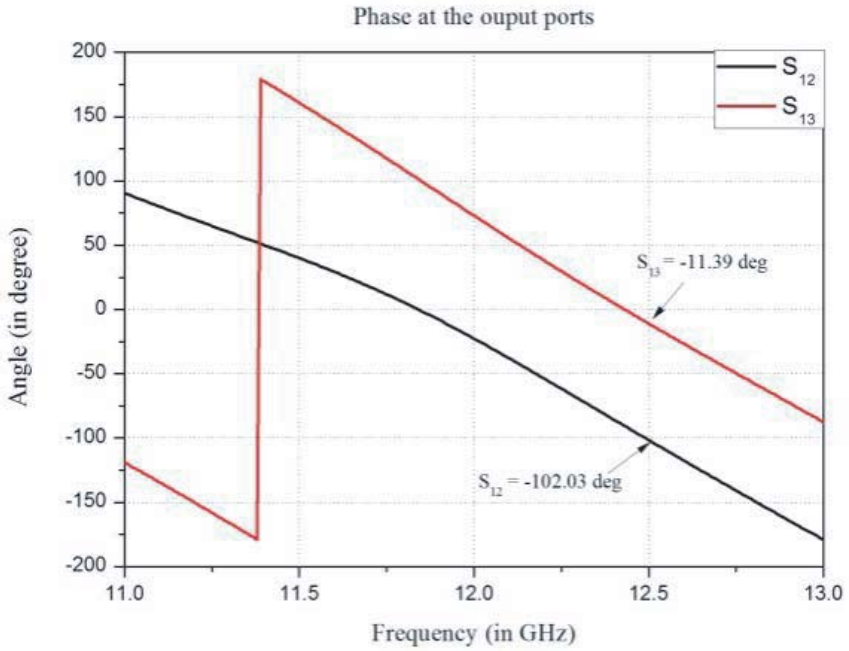

Figure 3. Phase at the output ports.

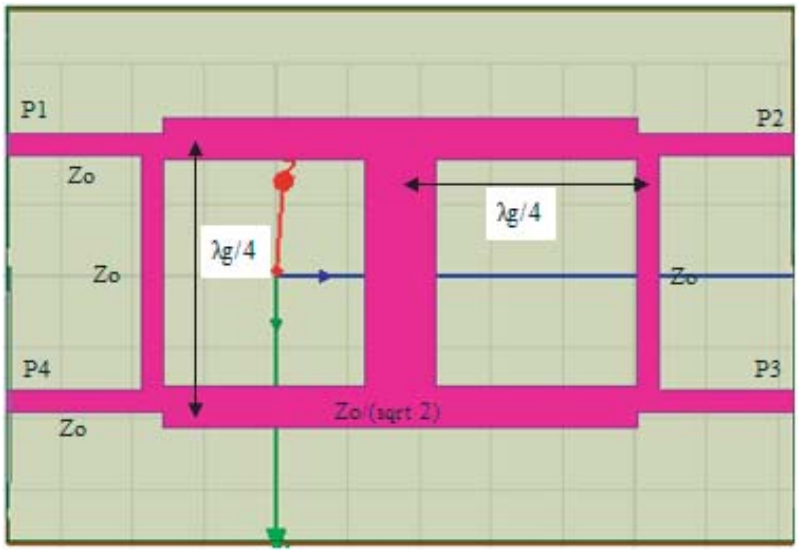

Figure 4. Layout of the 0 dB coupler.

The 0 dB coupler is designed and simulated in ANSYS HFSS to get the S-parameters. Figure 5 shows that the values of parameters S_{11}, S_{21}, S_{31}, and S_{41} are -20.11 dB, -14.34 dB, -1.40 dB, and -23.53 dB, respectively.

Thus, it can be interpreted from the values that when port 1 is used as the input port, then the adjacent ports 2 & 4 have no power to be transferred. It is also revealed that power has been transferred to only port 3. The phase angles between port 1 and port 3 is shown in Figure 6.

It is revealed from Figure 6 that the input port is at a phase of 137.55 deg while port 3 acting as the output port has a phase of 47.24 deg. Thus, a total phase difference of 90.31 deg between the input and output ports is obtained. Hence it can be seen from the results of the 0 dB coupler that the output port has a phase difference of 90° with the input port.

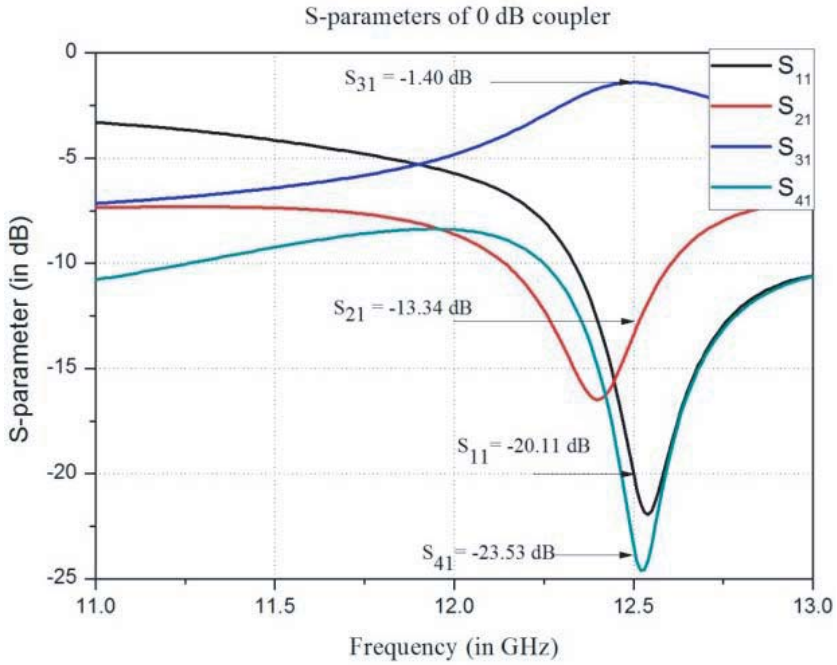

Figure 5. Magnitude of S-parameters of 0 dB coupler.

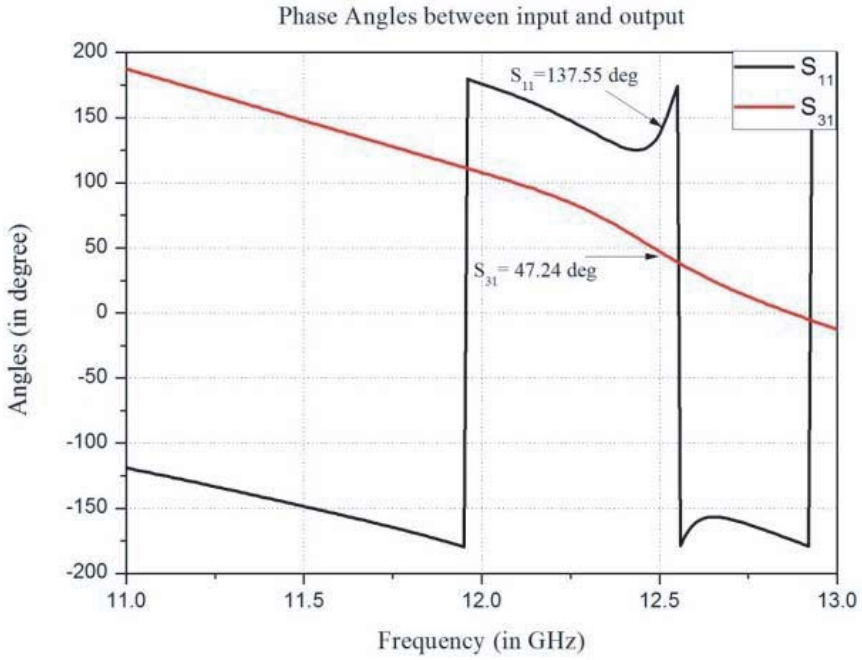

Figure 6. Phase angles between the input and output port of 0 dB coupler.

2.3. Phase Shifters

Phase shifters are also designed with the concept that a length of λ corresponds to a phase difference of 2π. Thus, by using this concept a transmission line of length L will provide a phase difference of

$$\emptyset = \frac{2\pi}{\lambda} L \tag{2}$$

where $\emptyset$ is the total phase difference obtained in radians, and λ is the wavelength. The wavelength λ is calculated from Equation (3)

$$\lambda = \frac{\lambda_o}{\sqrt{\in_{reff}}} \tag{3}$$

The following Figure 7 shows the transmission line used to make a phase difference.

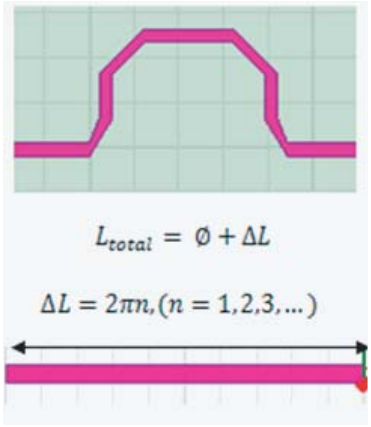

Figure 7. Layout of the phase shifter.

The phase shifter is designed in ANSYS HFSS, and Figure 8 shows the simulated phase output.

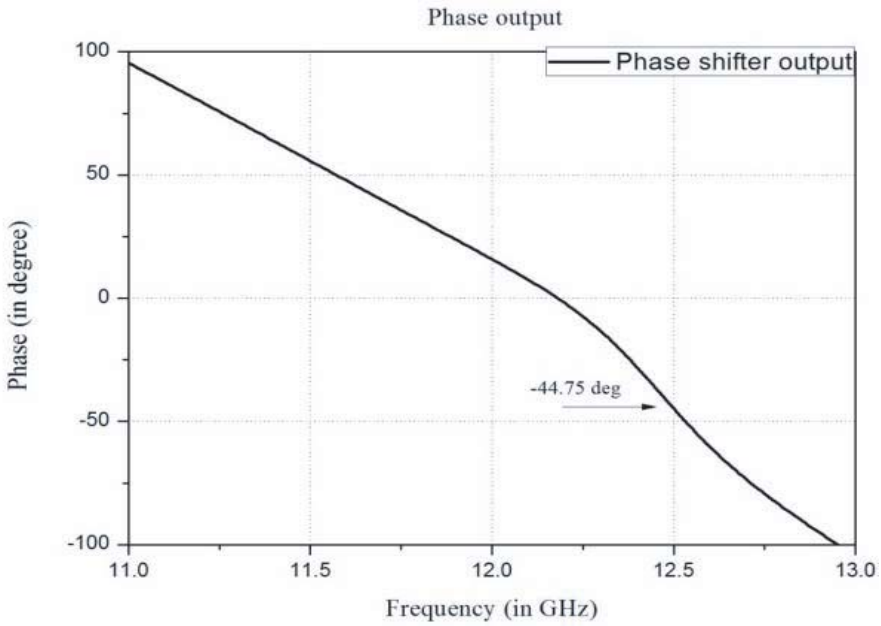

Figure 8. Phase output of the phase shifter.

3. BUTLER MATRIX DESIGN

A 4×4 Butler matrix has been designed using the 0 dB coupler, 3 dB coupler, and phase shifters to get power at different amplitudes and phases at the output of the matrix. Firstly, two 3 dB couplers have been designed which will serve as the input ports of the Butler matrix. The two outputs of the 3 dB couplers are used to feed the 0 dB coupler and phase shifter to provide the necessary phase shifts

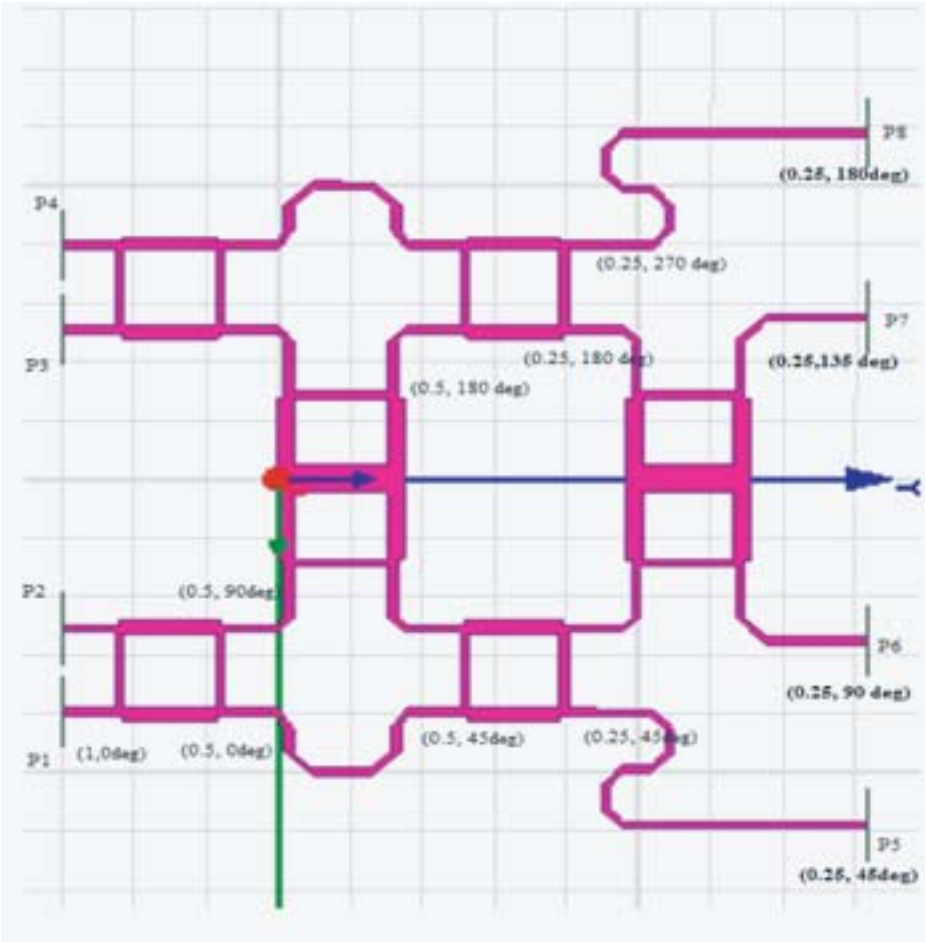

Figure 9. Layout of the 4×4 Butler matrix.

and change in the amplitude. The Butler matrix is designed in such a way that it divides the power amplitude in four equal parts, and the successive angles are $-45°$. The power division in the matrix is shown in Figure 9.

4. BUTLER MATRIX COMMUNICATION SYSTEM DESIGN PROCESS MODEL USING PETRI NETS

Here, a Butler matrix design system is presented (see Figure 12) in which process modelling of Butler matrix is done by Petri net (see Figure 13), and the model is analyzed and simulated in MATLAB. First, the process model, with dielectric constant of 10.2 and height of $h = 0.64\,\text{mm}$, resonates at a frequency of 12.50 GHz. The matrix being one of the most basic examples in microstrip design has been simulated on ANSYS HFSS (High Frequency Structure Simulator) software here, and for its process validations Petri net modelling has been used. Petri net is simply a graphical technique used to analyze and validate the concurrent and parallel processing. So for the validation of the design process used here, the Petri net modeling for analyzing the system processes is done.

4.1. Petri Nets

In this section, the basic definitions and properties related to Petri nets are discussed. The underlying structure of PNs is based on graphs. Graphs are mathematical structures which are used to model the relation between interconnected elements. Next, we discuss the mathematical definition of graphs and their different types [27, 28].

Definition 4.1: A Petri net is an algebraic structure $= \langle P, T, F, W \rangle$, where P is the set of conditions, and T is the set of events. These two sets are disjoint, but union is never empty. A flow relation $F \subseteq (P \times T) \cup (T \times P)$ is the set of lines, and W: $F \rightarrow \{1, 2 \ldots\}$ is the positive integer weight function. Petri net is an ordinary net if and only if W: $F \rightarrow \{1\}$, generally in model representation unity weight, is ignored, See Figure 10.

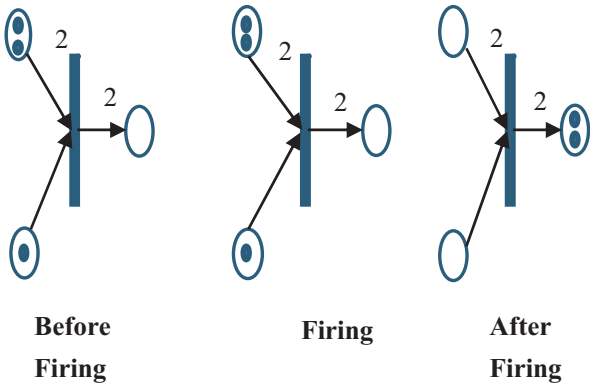

Figure 10. Sate after firing of Transition in Petri Net.

In a Petri net, a marking initially done by a function M_0: $P \rightarrow \{0, 1, 2 \ldots\}$ is used for the token's assignment for each place. Here $M_0(p)$ denotes the total number of commands in any condition p, at initial marking M_0. $M_0(p)$ is less than or equal to the capacity k of the place p, where capacity of the place is defined as k: $P \rightarrow \{1, 2, 3 \ldots\}$, and the capacity of a place is the maximum strength to accommodate the tokens at any reachable marking obtained from initial marking. Any initial marking is reachable to another marking M, if a firing sequence of transitions firing $\{t_1, t_2, \ldots, t_n\}$ occurs, such that M can occur from initial marking after firing of these transitions.

Definition 4.2: In a Petri net, a place p is said to be k-bounded if and only if number of tokens in place p, at initial marking, is always strictly less then k, where $k \in R^+$ [22, 23].

Definition 4.3: Any non-empty subset of places S is called a Siphon, if for every place p in S, the set of input transitions of place p is always a subset of the set of output transitions of p. Likewise, any non-empty subset of places Q is called a trap, if for every place p in Q, the set of output transitions of place p is always a subset of the set of input transitions of p [23].

Definition 4.4: A directed (undirected) graph or digraph G is defined as an ordered pair of a set of vertices or nodes V and a set of edges E, where each element of E is an ordered (unordered) pair consisting of two elements from set V (Figure 12). Graph is usually represented as $G = (V, E)$.

For each pair $(xy) \in E$, there is a line in G called as *edge or arc*, joining the vertices x and y. It is usually denoted by e. For digraph, the direction of an edge is given while the direction is absent in the case of undirected graph [22, 23].

Definition4.5: A graph $G = (VE)$ is called as a weighted graph when each edge e of the graph is assigned a number known as *weight*, w of the edge [22, 23].

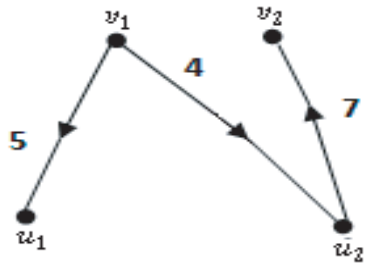

Figure 11. Directed, weighted, bipartite graph having two vertices set $V_1 = \{v_1 v_2\}$ and $V_2 = \{u_1 u_2\}$.

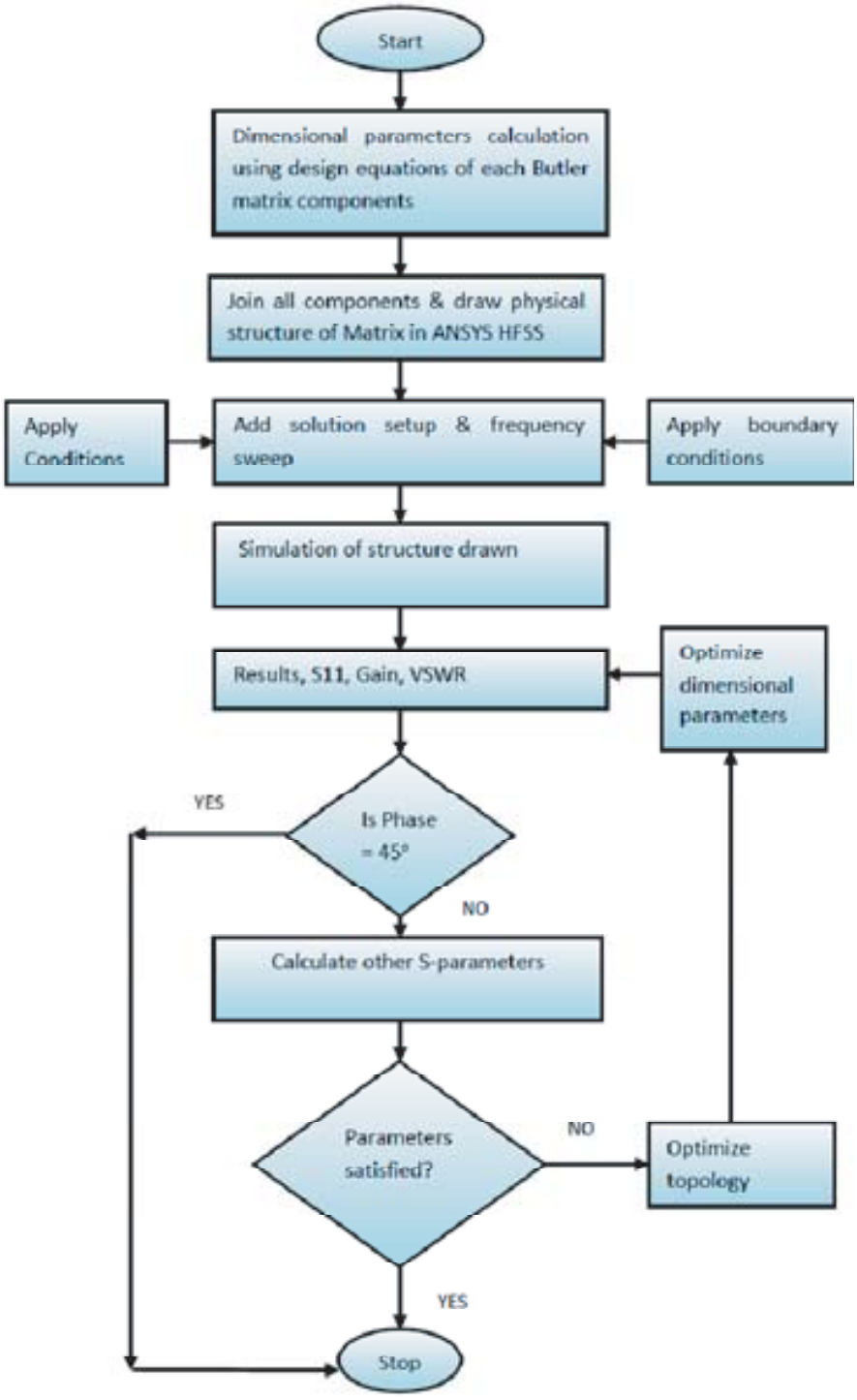

Figure 12. Design methodology of matrix.

Definition 4.6: A graph $G = (VE)$ is known as a bipartite graph if the vertex set V can be partitioned into two disjoint subsets V_1 and V_2 such that no edge in the graph G joins two vertices in V_1 or two vertices in V_2 (Figure 11) [22, 23].

4.2. Structural Analysis

The structural analysis of the Petri net model helps to determine certain structures which allow decisions on dynamic properties. The structural properties depend on the initial marking of the Petri net. The structural properties discussed in this paper will check whether the Petri net model is ordinary, bounded, consistent, and conservative, and what are the siphons and traps.

A Petri net is *ordinary* PN if all the arc weights are equal to one. If for every transition the sum of the input edge weights is equal to the sum of the weights of the output edges, the PN is *conservative*. In other words, in a conservative PN, the total number of tokens will remain constant. A conservative PN is *bounded*. A PN is said to be *consistent* if there exists a marking M' and a sequence s of firing transitions starting from M' back to M' such that each transition appears at least once in s. Siphons and traps also play a significant role in the structural analysis of Petri net model. A *siphon* N is a subset of places in an ordinary PN such that the set of input transitions of N is a subset of the set of output transitions of N. If any of the places in a siphon becomes token free, then that siphon will always remain unmarked. Similarly, a *trap* R is a subset of places in an ordinary PN such that the set

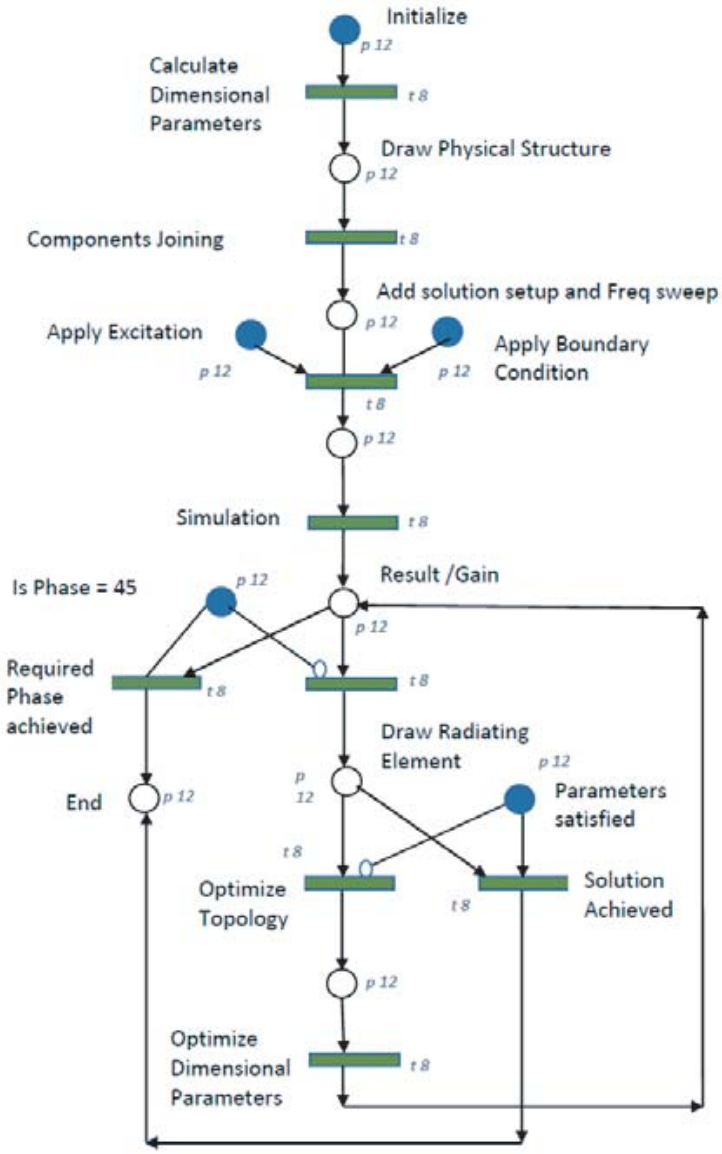

Figure 13. Petri Net model of design process of designing of radiating element array.

of output transitions of R is a subset of the set of input transitions of R which means that if any of the places in a trap contains a token, then that trap will never be empty.

4.3. Behavioral Analysis

The behavioral analysis of the PN model is done using behavioral properties (marking-dependent properties) of the Petri nets. Here, we will analyze two behavioral properties of the Petri nets — Liveness and Coverability tree.

A transition is *live*, if it can be fired in any marking. A Petri net is said to be *live* or in *deadlock-free* state, if it is possible to fire any transition through some firing sequence independent of the marking state. A marking M in a Petri net is said to be *coverable* if there exists a marking M'. The *coverability tree* will give the list of all the possible coverable markings represented as a tree. In a coverability tree, nodes represent generated markings; root represents the initial marking; and edges represent firing transition.

The developed radiating element array designing model based on Petri nets is shown in Figure 13. The tokens are initially placed in p1, p4, p5, p8, and p10. The tokens at places p4 and p5 denote necessary conditions. The token at position p8 denotes that the gain is enough while the token at position p10 shows that the parameters are satisfied. Description, arrangement of position, and transition of developed model are presented in Table 1 and Table 2, respectively.

Table 1. Description of positions of array design model.

Position	***Description***
P 1	*Model starting position*
P 2	*Designing physical structure with details about feeding technique*
P 3	*Add solution setup and frequency sweep as per the requirement*
P 4	*The token at this place indicates that the excitation is applied*
P 5	*The token present at this place indicates that boundary conditions are applied*
P 6	*This position indicates the process of finding gain VSWR and S parameters*
P 7	*Results as parameters and gain are calculated*
P 8	*A buffer position intended to check whether gain is sufficient or not*
P 9	*Draw array and feed structure*
P 10	*A buffer position intended to check whether parameters are satisfied or not*
P 11	*Position for indication of necessity to change the physical parameter*
P 12	*Model completion position*

4.4. Properties Validation of Communication System Design

The PN model for design process can be constructed in PN Toolbox in MATLAB as shown below in Figure 14.

The incidence matrix for further mathematical analyses can be calculated as shown below in Figure 15.

The model is found to be live as shown in Figure 16, which means that each transition is fired at least once, and therefore, each state is significant in this model.

The cover-ability tree explaining the movement from one state to another can be made in graphic mode using PN Toolbox as shown in Figure 17. It demonstrates that every state in this model is finite and feasible, and represents non-presence of any deadlock or undefined situations.

As can be seen in Figure 18 and Figure 19, the model is not only conservative but also consistent, i.e., no tokens are consumed during the process.

Table 2. Description of transitions of array design model.

Transition	***Meaning***
T 1	*Calculate physical parameters using design equations of single element*
T 2	*Physical structure evaluation*
T 3	*Solution setup and frequency sweep*
T 4	*Electrodynamic analysis using FEM in HFSS*
T 5	*Required gain achieved*
T 6	*Parametric analysis*
T 7	*Optimized topology*
T 8	*Got required solution*
T 9	*Optimized physical parameters*

5. RESULT AND DISCUSSIONS

The design has been simulated in ANSYS HFSS and then fabricated to get the results. The hardware design of the matrix is shown in Figure 20.

The Butler matrix is then tested for the S-parameter results and compared with the simulation results to confirm them. Port 1 is taken as the input port, and then testing is done for every port. It is revealed from Figure 21 that the S_{11} parameter resonates at 12.5 GHz with a magnitude of -33.33 dB while the measured value is -16.36 dB. The difference in the results may be accounted due to some fabrication error and surrounding interference from the wave present. This difference being large still satisfies the goal of keeping S_{11} below -10 dB theoretically and -15 dB practically [8].

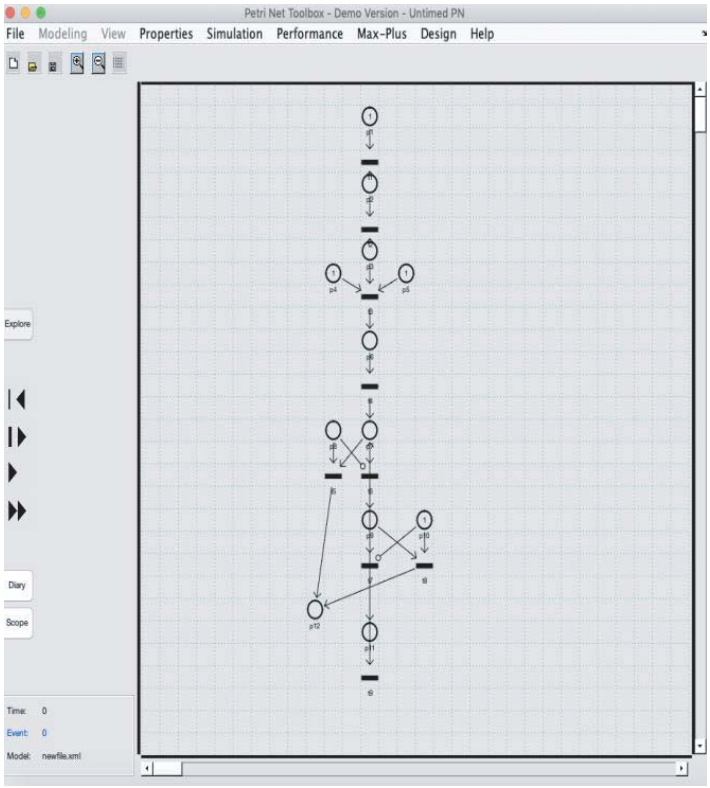

Figure 14. PN Model for design process.

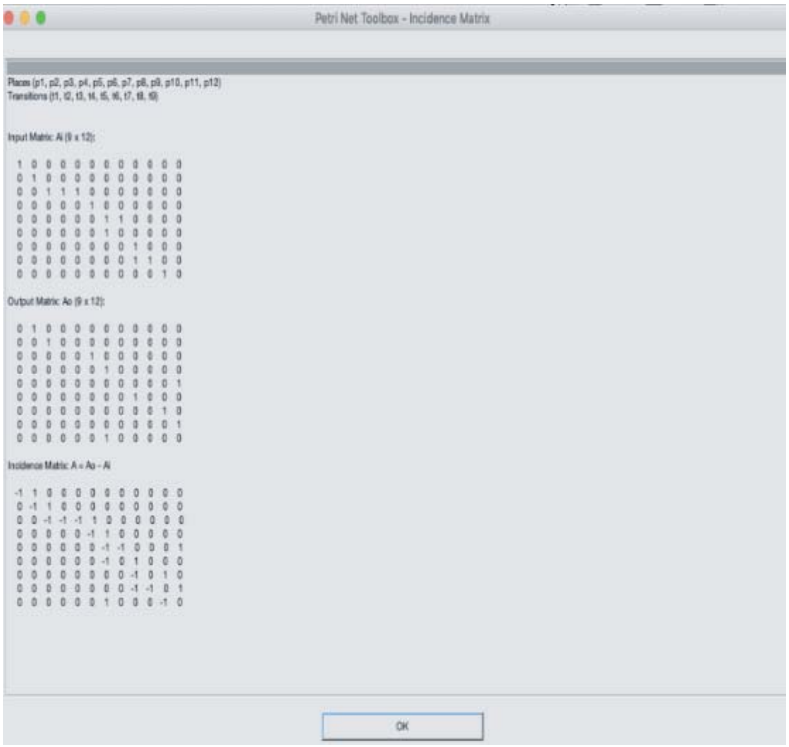

Figure 15. Incidence matrix for design process.

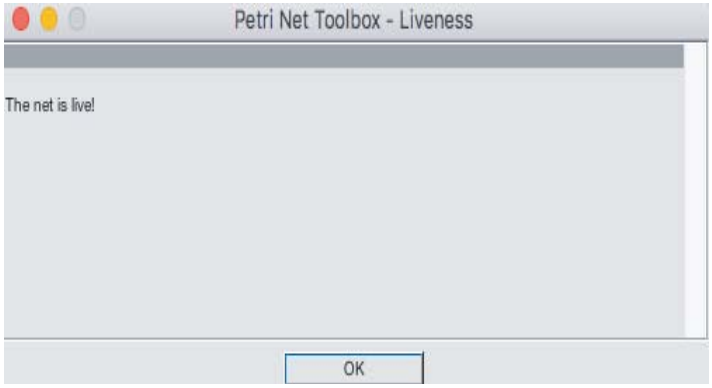

Figure 16. Liveness of PN base model for design process.

Table 3. Comparison of simulated and measured results.

Parameter	Magnitude (in dB)		Phase (in degree)	
S-Parameters	**Simulated**	**Measured**	**Simulated**	**Measured**
S_{11}	−33.33	−16.36	−−	−−
S_{15}	−6.89	−6.81	*43.37*	*43.27*
S_{16}	−3.29	−3.67	*88.99*	*88.41*
S_{17}	−3.67	−4.02	*132*	*134.3*
S_{18}	−3.41	−3.44	*179.9*	*179.30*

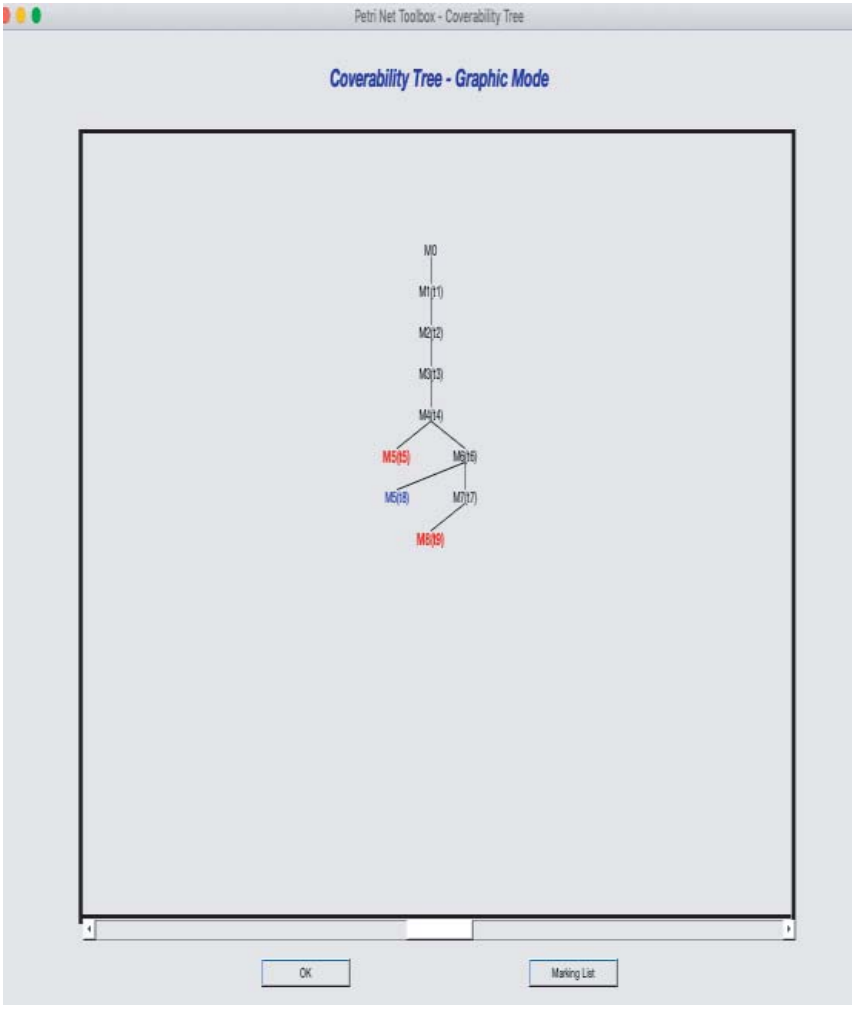

Figure 17. Cover-ability Tree of PN base model for design process.

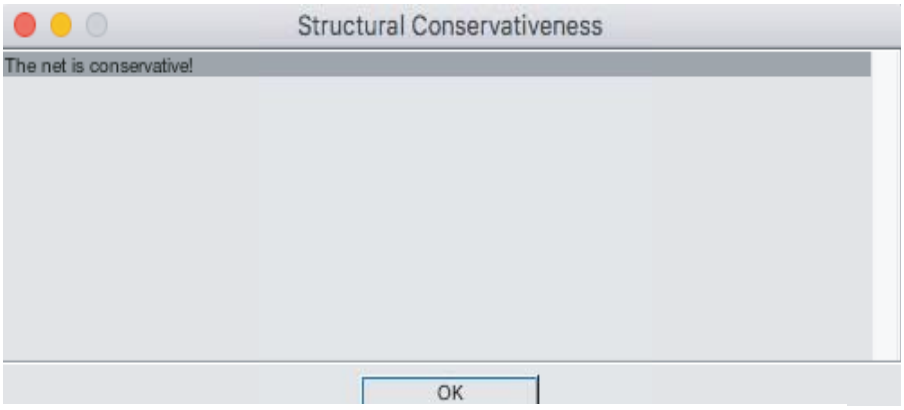

Figure 18. Conservativeness of PN base model for design process.

The simulated and measured results are shown in a tabular form in Table 3.

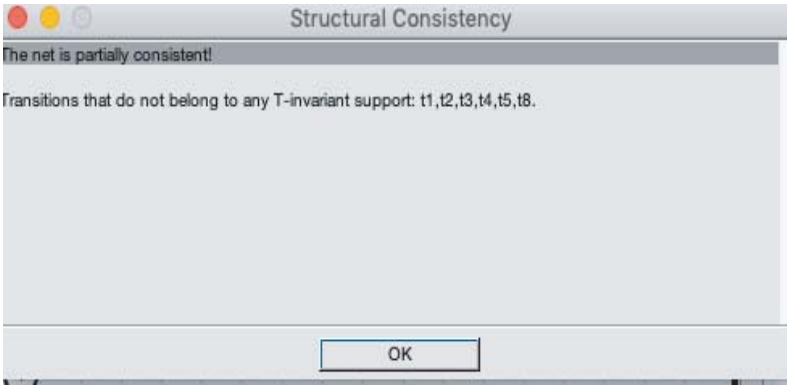

Figure 19. Consistency of PN base model for design process.

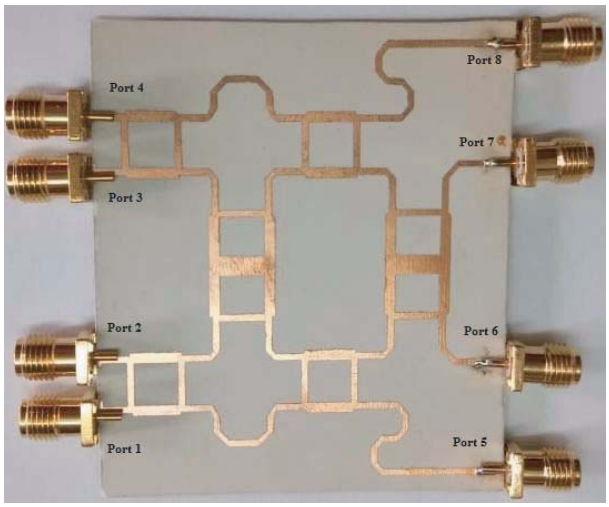

Figure 20. Fabricated Butler matrix.

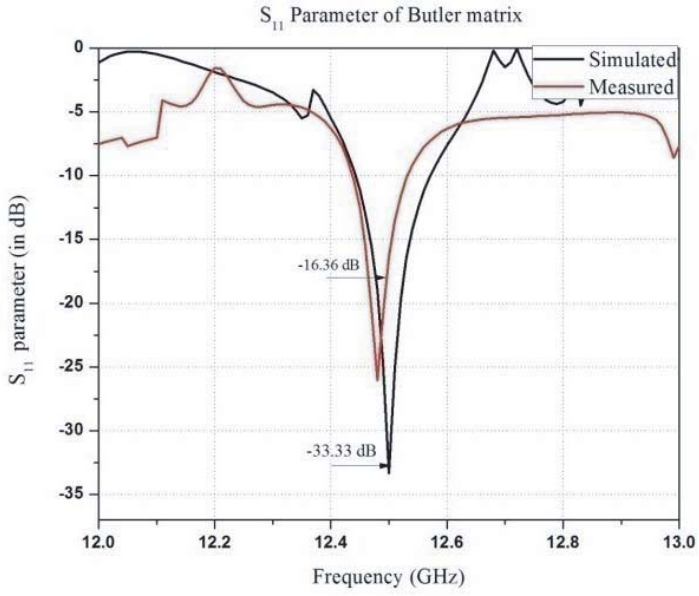

Figure 21. Simulated and measured S_{11}-parameter.

6. CONCLUSION

In this paper, Petri net is used for better understanding the design process of a phase array system. Firstly, the process is represented graphically, and then it is analyzed for designing and removing any deadlocks in the process. For this, some important properties like live-ness and coverability tree are used as they explain very well the working process running and establish relation between previous stages and current stage so that we can remove the deadlocks, occurring during designing process. For applying this Petri net technique for phase array system, a 4×4 Butler matrix is designed which provides a progressive phase difference of 45°, and power is divided into four equal parts. It has myriad applications in wireless communication system like satellites and aircraft applications. This matrix can be used to feed the antenna system which can be attached to its output ports. Thus, we can have four antennas which are provided with equal power, and phase is separated by a phase of 45°. The matrix along with the antenna further can be used as a phase array for satellites applications. For validation of design process, Petri net is introduced for analyzing structural and behavioral properties of the system design for better understanding. Researchers can add the same concept for validations of design processes for various array designs, structures, multi-feed and their applications in the IEEE standard bands like patches, filtering array, array using Butler matrix for indoor wireless environment, arrays for biomedical and RF harvesting, and broadband mobile communication. It can help in network parameters selection using deadlock condition removal by converting Petri net into stochastic Petri net and timed Petri net by associating certain time interval for each transition or process of the system for improving their antenna energy efficiency.

REFERENCES

1. El-Tager, A. M. and M. A. Eleiwa, "Design and implementation of a smart antenna using Butler matrix for ISM-band," *Progress In Electromagnetics Research Symposium*, Beijing, 2009.
2. Kilani, M. B., M. Nedil, N. Kandil, and T. A. Denidni, "Design of conformal microstrip Butler matrix at 2.4 GHz," *IEEE International Symposium on Antennas and Propagation*, Chicago, 2012.
3. Alam, M. M., "Microstrip antenna array with four port Butler matrix for switched beam base station application," *12th International Conference on Computer and Information Technology (ICCIT)*, Dhaka, 2009.
4. Pandey, A. K., "Design of a compact high-power phased array for 5G FD-MIMO system at 29 GHz," *Asia-Pacific Microwave Conference*, New Delhi, 2016.
5. Babale, S. A., S. K. A. Rahim, O. Elijah, and S. I. Orakwue, "Two-dimensional beam-steering phased-array utilizing 2×2 Butler matrix," *IEEE 3rd International Conference on Electro-Technology for National Development (NIGERCON)*, Owerri, Nigeria, 2017.
6. Ding, K., X. Fang, Y. Wang, and A. Chen, "Printed dual-layer three-way directional coupler utilized as 3×3 beamforming network for orthogonal three-beam antenna array," *IEEE Antennas and Wireless Propagation Letters*, Vol. 13, 911–914, 2014.
7. Solmain, I., A. Rydosz, S. Gruszczynki, and K. Wincza, "Three beam microstrip antenna arrays fed by 3×3 Butler matrix," *7th IEEE International Symposium on Microwave, Antenna, Propagation, and EMC Technologies (MAPE)*, Xi'an, China, 2017.
8. Djera, T., N. J. G. Fonseca, and K. Wu, "Design and implementation of a planar 4×4 Butler matrix in SIW technology for wide band high power applications," *Progress In Electromagnetics Research B*, Vol. 35, 29–51, 2011.
9. Zhai, Y., X. Fang, K. Ding, and F. He, "Miniaturization design for 8×8 Butler matrix based on back-to-back bilayer microstrip," *International Journal of Antennas and Propagation*, Vol. 2014, 1–7, 2014.
10. Rosati, G. and J. Munn, "Fast prototyping of an 8×8 Butler matrix beamforming network for 5G applications," *International Conference on Electromagnetics in Advanced applications, (ICEAA)*, Verona, Italy, 2017.

11. Lei, S. and L. Jian, "Beam forming networks for triangular grid multi-beam array," *IEEE International Conference on Microwave Technology & Computational Electromagnetics*, Qingdao, China, 2013.
12. Zulkifli, F. Y., N. Chasanah, and E. T. Rahardjo, "Design of Butler matrix integrated with antenna array for beam forming," *International Symposium on Antennas and Propagation (ISAP)*, Hobart, Australia, 2015
13. Zhou, C., J. Fu, H. Sun, and Q. Wu, "A novel compact dual-band Butler matrix design," *3rd Asia-Pacific Conference on Antennas and Propagation*, Harbin, China, 2014.
14. Lazović, L., A. Jovanović, B. Lutovac, and V. Rubežić, "The application of graph theory for the design of reconfigurable fractal antenna," *2016 24th Telecommunications Forum (TELFOR)*, Belgrade, Sweden, 2016.
15. Prakash, V., S. Kumawat, and P. Singh, "Circuital analysis of coaxial fed rectangular and U-slot patch antenna," *International Conference on Computing, Communication and Automation (ICCCA2016)*, Greater, Noida, 2016.
16. Prakash, V., S. Kumawat, and P. Singh, "Design and analysis of full and half mode substrate integrated waveguide planar leaky wave antenna with continuous beam scanning in X-Ku band," *Frequenz*, Vol. 73, No. 5, 171–178, 2019.
17. Ren, H., B. Arigong, M. Zhou, J. Ding, and H. Zhang, "A novel design of 4×4 Butler matrix with relatively flexible phase differences," *IEEE Antennas and Wireless Propagation Letters*, Vol. 15, 1277–180, 2016.
18. Wang, W., Z. Qu, Z. Shen, L. Lou, K. Tang, and Y. Zheng, "Design of broadband phased array antenna at X-band," *2017 Progress In Electromagnetics Research Symposium — Fall (PIERS — FALL)*, Singapore, Singapore, Nov. 19–22, 2017.
19. Chu, H. N. and T.-G. Ma, "An extended 4×4 Butler matrix with enhanced beam controllability and widened spatial coverage," *IEEE Transactions on Microwave Theory and Techniques*, Vol. 66, No. 3, 1301–1311, 2018.
20. Yao, Y.-L., F.-S. Zhang, and F. Zhang, "A new approach to design circularly polarized beam-steering antenna arrays without phase shift circuits," *IEEE Transactions on Antennas and Propagation*, Vol. 66, No. 5, 2354–2364, 2018.
21. Murata, T., "Petri nets: Properties, analysis and applications," *Proceedings of the IEEE*, Vol. 77, 541–580, 1982.
22. Kumawat, S. and G. N. Purohit, "Total span of farm workflow using Petri net with resource sharing," *Int. J. Business Process Integration and Management*, Vol. 8, 160–171, 2017.
23. Kumawat, S., "Weighted directed graph: A Petri Net based method of extraction of closed weighted directed Euler trail," *International Journal of Services, Economics and management*, Vol. 4, No. 3, 252–264, 2012.
24. Shareef, A. and Y. Zhu, "Effective Stochastic modelling of energy constrained wireless sensor networks," *Journal Computer Network and Communication*, 2012.
25. Di Martino, C., "Resiliency assessment of wireless sensor networks: A holistic approach," Ph.D. Thesis, Federico II, University of Naples, Italy, 2009.
26. Yahya, B., J. Ben-Othman, L. Mokdad, and S. Diagne, "Performance evaluation of a medium access control protocol for wireless sensor networks using Petri Nets," *HET-NET's 2010*, 335–354, 2010.
27. Gupta, S., S. Kumawat, and G. P. Singh, "Fuzzy Petri Net representation of fuzzy production propositions of a rule based system," *Communications in Computer and Information Science, Springer CCIS, Advances in Computing and Data Sciences*, 197–210, 2019.
28. Gupta, S., G. P. Singh, and S. Kumawat, "Petri Net recommender system to model metabolic pathway of polyhydroxyalkanoates," *International Journal of Knowledge and Systems Science (IJKSS) IGI Global Editorial Discovery*, Vol. 10, No. 2, 18, 2019.